

# Various Dendritic Abnormalities Are Associated with Fibrillar Amyloid Deposits in Alzheimer's Disease

JAIME GRUTZENDLER,<sup>a,b</sup> KATHRYN HELMIN,<sup>a</sup> JULIA TSAI,<sup>a</sup>  
AND WEN-BIAO GAN<sup>a</sup>

<sup>a</sup>*Skirball Institute of Biomolecular Medicine, Department of Physiology and Neuroscience, New York University School of Medicine, New York, New York, USA*

<sup>b</sup>*Current address: Northwestern University, Chicago, Illinois, USA*

**ABSTRACT:** Dystrophic neurites are associated with fibrillar amyloid deposition in Alzheimer's disease (AD), but the frequency and types of changes in synaptic structures near amyloid deposits have not been well characterized. Using high-resolution confocal microscopy to image lipophilic dye-labeled dendrites and thioflavin-S-labeled amyloid plaques, we systematically analyzed the structural changes of dendrites associated with amyloid deposition in both a transgenic mouse model of AD (PSAPP) and in human postmortem brain. We found that in PSAPP mice, dendritic branches passing through or within 40  $\mu\text{m}$  from amyloid deposits displayed various dendritic abnormalities such as loss of dendritic spines, shaft atrophy, bending, abrupt branch endings, varicosity formation, and sprouting. Similar structural alterations of dendrites were seen in postmortem human AD tissue, with spine loss as the most common abnormality in both PSAPP mice and human AD brains. These results demonstrate that fibrillar amyloid deposits and their surrounding microenvironment are toxic to dendrites and likely contribute to significant disruption of neuronal circuits in AD.

**KEYWORDS:** Alzheimer's disease, AD, amyloid plaques, dendrite

## INTRODUCTION

Alzheimer's disease (AD) is a progressive neurodegenerative disease that is pathologically characterized by the accumulation of amyloid- $\beta$  peptide ( $A\beta$ ) and neurofibrillary tangles in susceptible brain regions.<sup>1-10</sup> Many lines of

Address for correspondence: Wen-Biao Gan, New York University School of Medicine, 540 First Avenue, Skirball 5-4, New York, NY 10016. Voice: 212-263-2585; fax: 212-263-8214.  
gan@saturn.med.nyu.edu

*Ann. N.Y. Acad. Sci.* 1097: 30–39 (2007). © 2007 New York Academy of Sciences.  
doi: 10.1196/annals.1379.003

evidence suggest that synapse loss occurs early and progressively in the pathogenesis of AD and is closely associated with the duration and severity of cognitive impairment in AD patients.<sup>11–17</sup> The accumulation of both diffusible and fibrillar forms of A $\beta$  has been linked to functional and structural synaptic alterations, contributing to the cognitive decline seen in AD. The presence of elevated levels of soluble A $\beta$  peptides has been shown to lead to a reduction in long-term potentiation, as well as deficits in learning and memory that occur even before amyloid plaque formation.<sup>18–25</sup> In addition, the deposition of fibrillar amyloid has been associated with various morphological changes in synaptic structures. Electron microscopy studies in human AD tissue and transgenic mouse models have revealed dystrophic neurites surrounding the amyloid deposits,<sup>26,27</sup> while Golgi and immunocytochemical staining have shown aberrant neuritic sprouting near amyloid plaques.<sup>28–31</sup> Neuronal processes located near plaques exhibit increased curvature or tortuosity, and such distortion in neurite geometry has been implicated in the dysfunction of neuronal circuitry.<sup>32–34</sup> Recent studies in a mouse model of AD have shown that dendrites located near amyloid deposits exhibit local spine loss and shaft atrophy that may eventually lead to dendrite breakage, indicating that the deposition of fibrillar amyloid could contribute significantly to the progression of AD.<sup>35</sup>

In this study, we examined the frequency and types of dendritic structural abnormalities within and near amyloid deposits in a transgenic mouse (PSAPP) model of AD<sup>36,37</sup> as well as in human postmortem AD brain. We found several dendritic abnormalities, including spine loss, shaft atrophy and bending, branch breakage, and sprouting. In both PSAPP mice and human AD brain, dendritic spine loss was the most frequently seen structural abnormality in the vicinity of amyloid deposits. These results indicate that synaptic disruption is a prominent feature associated with fibrillar amyloid plaques and underscores the potential importance of therapies aimed at preventing or removing amyloid deposits in AD.

## METHODS

### *Experimental Animals*

Transgenic mice overexpressing mutant human amyloid precursor protein (Tg2576) and mutant human presenilin 1 (PS1<sub>M146L</sub>) were obtained from Dr. Karen Duff at the Nathan Klein Institute at New York University.<sup>38</sup> Mice of 4 to 7 months of age were anesthetized with pentobarbital (80 mg/kg) and perfused transcardially with 40 mL of 4% paraformaldehyde. Brains were dissected out and postfixed for 10 min in 4% paraformaldehyde before slicing. Transversal slices (150–200  $\mu$ m thick) at the level of the hippocampus were cut on a vibratome (Vibratome 1000, TPI Inc., St. Louis, MO) and were subjected to labeling.

### *Postmortem Human Brain*

The brains from two patients with a diagnosis of AD were obtained within 24 h postmortem. Small hippocampal and frontal lobe blocks were immediately placed in 4% paraformaldehyde for less than 12 h and then stored in PBS until the time of sectioning. Tissue slices of 200  $\mu\text{m}$  were obtained with a vibratome prior to labeling.

### *Labeling of Neurons*

Neuronal structures were labeled with the DiOlistic technique as previously described.<sup>39</sup> Briefly, 3 mg of lipophilic dye DiI were dissolved in 100  $\mu\text{l}$  of methylene chloride (Sigma, St. Louis, MO). The solution was used for coating a small amount (100 mg) of tungsten particles (1.5  $\mu\text{m}$  diameter) (Bio-Rad, Hercules, CA) with the dye. Tungsten particles were introduced into Tefzel tubing (Bio-Rad cat 165-2441) for the preparation of “bullets.” Dye-coated particles were delivered to the preparation using a commercially available biolistic device, a “gene gun” (Bio-Rad, Helios Gene Gun System). Tissues were protected from the air shock wave by interposing a membrane filter with a 3- $\mu\text{m}$  pore size (Millipore cat TSTP04700) between the gun and the tissue. After particle delivery, the dye was allowed to diffuse for >24 h prior to mounting and imaging.

### *Staining of Fibrillar Amyloid Deposits*

Following lipophilic dye labeling, fibrillar amyloid deposits (neuritic plaques) were stained for 10 min in a solution of thioflavin-S (2  $\mu\text{g}/\text{mL}$ , Sigma, cat T-1892) in 0.1 M PBS and then rinsed with 0.1 M PBS.

### *Imaging of Neuronal Structures*

Images of labeled neurons were acquired by a Zeiss LSM 510 confocal attached to an upright Zeiss Axioplan 2 microscope. Neurons were viewed under a 40X/1.30 oil immersion DIC Plan-Neuofluar objective. Neuronal structures labeled with DiI were sequentially scanned using the appropriate excitation lasers (458 nm for thioflavin S and 543 nm for DiI) combined with the appropriate emission filter (LP 560 for DiI and BP475-525 for thioflavin S). Stacks of images at 0.3–1.0- $\mu\text{m}$  steps were acquired to generate a three-dimensional data set of imaged neurons.

### *Quantification of Spine Density, Dendritic Diameter, and A $\beta$ Concentration*

Dendritic spine densities, dendritic diameters, and thioflavin-S labeling intensity profiles (a correlate of fibrillar A $\beta$  deposit) were quantified with Metamorph software (Universal Imaging Corporation, Downingtown, PA) as described in Tsai *et al.*<sup>35</sup> Each dendrite was divided into 6- $\mu$ m segments and spines were counted and diameters measured for each segment. Dendrites are considered exhibiting spine loss or shaft atrophy if they contain segments with more than 15% reduction in spine density or shaft diameter near amyloid deposits as compared to the adjacent segments of the same dendrites. Spine density was normalized to the spine density of segments in the same dendritic branch immediately adjacent to the segment passing through the amyloid deposit.

## RESULTS

We first examined the characteristics and frequency of structural dendritic alterations in a transgenic mouse model overexpressing mutant human amyloid precursor protein (APP) and mutant presenilin-1 (PS1) (PSAPP).<sup>36,37</sup> These mice begin to develop amyloid plaques at around 10 weeks of age and had large-scale deposition by 6 months of age.<sup>38</sup> Fixed hippocampal and cortical slices from PSAPP mice between 4 to 7 months of age were labeled by ballistic delivery of lipophilic dyes (DiOlistic technique), which labels neuronal dendrites in a Golgi-like manner (FIG. 1A).<sup>39,40</sup> Fibrillar amyloid deposits were labeled with thioflavin-S and dendrites in and around these deposits were visualized using high-resolution confocal microscopy.

We found that dendrites passing through or near fibrillar amyloid deposits showed various abnormalities including spine loss, dendritic shaft atrophy and bending, abrupt branch ending within and near deposits, branch sprouting, and varicosity formation (TABLE 1). Spine loss and shaft atrophy were observed, respectively, in 41% (101/244) and 24% (58/244) of dendrites passing through or within 40  $\mu$ m of amyloid deposits (FIG. 1B, C; see METHODS). Overall, dendritic segments within amyloid deposits showed  $\sim$ 40% reduction in spine density and  $\sim$ 20% reduction in shaft diameter as compared to those outside deposits.<sup>35</sup> Consistent with previous studies,<sup>20,41</sup> we found that dendrites closely surrounding or inside fibrillar deposits were more likely to exhibit shaft bending (FIG. 1A-B). Within  $\sim$ 40  $\mu$ m from the edge of deposits, over half of the dendrites curved around deposits as if being displaced from their original locations. Furthermore, 34% of dendrites (16/47) passing through deposits displayed single or multiple sharp bends (TABLE 1).

The fourth most frequently encountered dendritic abnormality was abrupt ending of dendrites near or within amyloid deposits (FIG. 1B; TABLE 1).<sup>35</sup> This

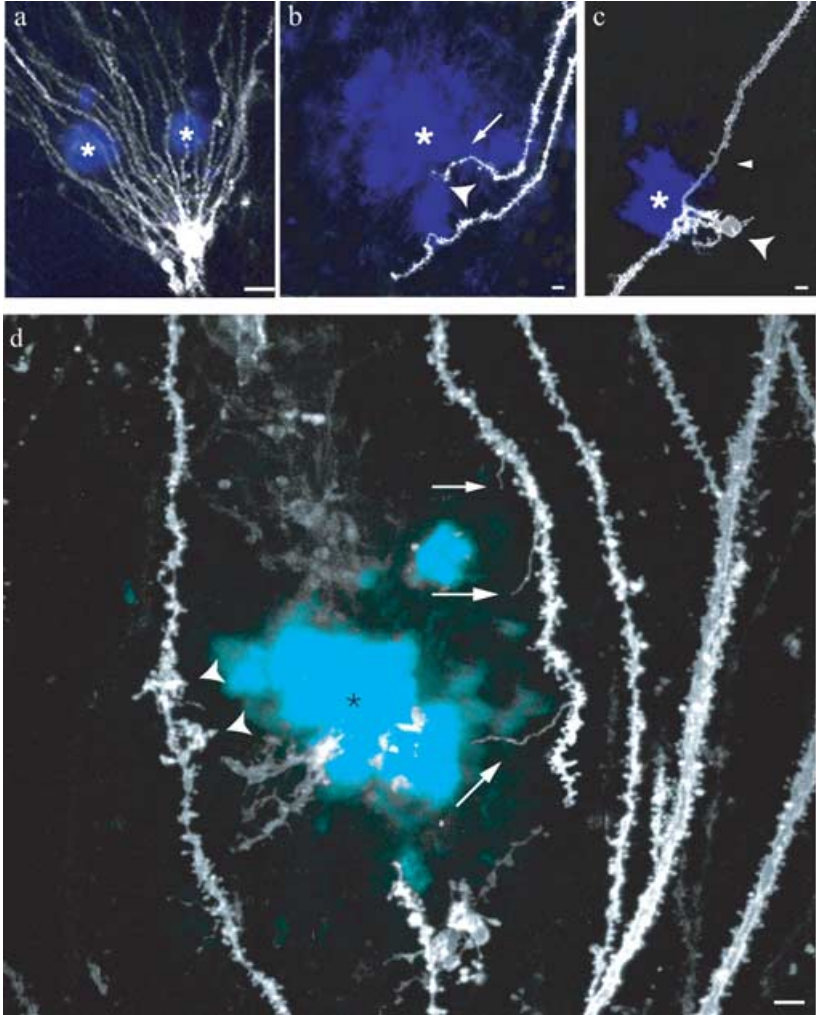


**FIGURE 1.** Dendritic structural abnormalities seen near fibrillar amyloid deposits in PSAPP mice labeled with the DiOlistic technique. **(A)** A cell with dendrites bending around amyloid deposits. **(B)** Dendrite abruptly ending inside an amyloid deposit (arrowhead), as well as spine loss and dendritic atrophy (arrow). **(C)** Dendritic varicosity near amyloid deposit (arrowhead) and spine loss and dendritic atrophy (arrow). **(D)** Dendritic sprouting near plaque (arrows), bending around plaque, and small varicosities (arrowheads). Amyloid deposits are marked with asterisks. Scale bars, 10  $\mu\text{m}$  for A and 5  $\mu\text{m}$  for B–D.

finding suggests that amyloid deposits may induce the breakage of nearby dendrites, consistent with previous results from *in vivo* imaging studies.<sup>35</sup> Occasionally, some dendritic shafts near deposits (5%; 12/244 dendrites) exhibited sprouting (unusually long, thin processes that do not resemble typical

**TABLE 1. Frequency of dendritic abnormalities within 40  $\mu\text{m}$  of fibrillar amyloid deposits in PSAPP mice<sup>a</sup>**

Abnormality	Frequency (number of dendrites)	Percentage of dendrites (%)
Spine loss	101/244	41
Sharp bending within plaques	16/47	34
Shaft atrophy	58/244	24
Abrupt ending	31/244	13
Sprouting	12/244	5
Varicosities	3/244	1

<sup>a</sup> $n = 4$  animals.

*Note:* A total of 244 dendrites from 4 PSAPP animals were examined for various dendritic abnormalities. In the case of sharp bending within plaques, only those dendrites passing through plaques ( $n = 47$  dendrites, 4 PSAPP animals) were used.

dendritic spines; FIG. 1D). Sprouting dendrites were found concurrently with other abnormalities, such as abruptly ending dendrites, suggesting that sprouting could occur as a compensatory mechanism following dendritic breakage.

A rare but occasional amyloid deposit-associated abnormality was the presence of dendritic varicosities (1%; 3/244 dendrites; FIG. 1C), which in contrast are seen very frequently in axons near amyloid plaques.<sup>35</sup> Axonal varicosities have been shown to contain large numbers of clustered vesicles that can be labeled by antibodies against presynaptic proteins.<sup>42</sup> Lack of synaptic vesicles could explain why dendrites are much less prone to varicosity formation.

To determine whether fibrillar amyloid deposits in human AD brain are associated with similar dendritic abnormalities as those in PSAPP transgenic mice, we analyzed dendrites in slices obtained post mortem from the frontal cortices and hippocampi of two elderly patients with a diagnosis of AD. Confocal microscopy of lipophilic dye-labeled dendrites passing through thioflavin-S positive amyloid deposits revealed several dendritic abnormalities similar to those seen in transgenic PSAPP mice. On average, we observed a 23% reduction in dendritic spine density ( $n = 120$  dendrites near 52 plaques;  $P < 0.05$ ) on segments passing through or up to 15  $\mu\text{m}$  from the thioflavin-S-positive plaques when compared to the immediately adjacent dendritic segments from the same dendritic branch outside of the plaque (FIG. 2A–C). Approximately 35% of these dendritic segments displayed at least a 15% reduction in spine density. Because of the large variability in spine density in different dendrites and regions in human tissue, we did not quantify spine density in dendritic branches that were not in the vicinity of plaques. In addition to spine loss, dendritic varicosities and sprouting were also occasionally (1–2% of dendrites) seen near plaques (FIG. 2C). However, in contrast to PDAPP mice, no obvious dendritic shaft atrophy or breakage was seen in the 120 dendrites observed (FIG. 2D).

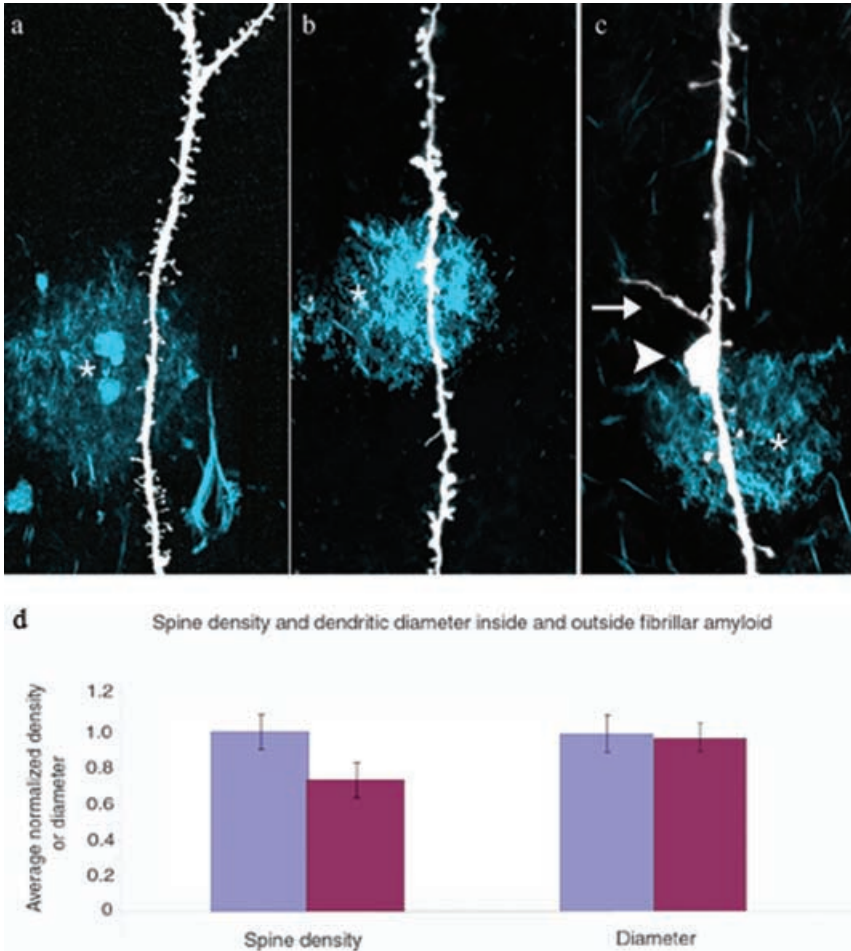


**FIGURE 2.** Dendritic structural abnormalities seen near fibrillar amyloid deposits in postmortem human AD brain. (A–B) Lipophilic dye-labeled dendrites passing through thioflavin-S-positive amyloid plaques show decreased spine density inside amyloid deposits. (C) Varicosity (*arrowhead*) and sprouting (*arrow*) on a dendrite passing through an amyloid plaque. (D) A 23% decrease in spine density is seen on dendritic segments passing through amyloid deposits (*dark gray bars*) when compared to adjacent segments on the same dendrite but outside the amyloid plaque (*light gray bars*); no significant difference in dendrite diameter is seen. Amyloid deposits are marked with asterisks.

## DISCUSSION

The accumulation of amyloid- $\beta$  peptide in susceptible brain regions is one of the pathological hallmarks of Alzheimer's disease.<sup>1–10</sup> To better understand the impact of amyloid deposition on the process of neuronal circuit disruption in

AD, we examined the type and frequency of dendritic structural abnormalities in a transgenic mouse model of AD (PSAPP) and in postmortem human AD tissue. Spine loss, shaft atrophy, and dendritic bending were the most common abnormalities seen in PSAPP mice, with abnormalities such as dendritic breakage, sprouting, and varicosities seen less frequently. In the human AD brain, spine loss was the most common abnormality, but sprouting and varicosities were also occasionally seen.

Overall dendritic structural changes are much more marked in PSAPP mice than in the human brain. These differences may be due to the fact that amyloid deposition in mice is likely to accumulate much more rapidly. Despite the lower degree of dendritic toxicity in humans, the detrimental effect of amyloid deposition could last over the much longer life span of a human and therefore may have a large cumulative effect on neuronal circuit disruption.

These studies demonstrate that fibrillar amyloid deposits and/or the microenvironment that surrounds them have a toxic effect on dendrites leading to the elimination of spines. This effect is highly local, suggesting that signals derived either from the amyloid deposits and/or the surrounding glial cells are responsible for the damage. Accumulation of soluble amyloid peptides could be the primary event in generating various dendritic abnormalities. Alternatively, fibrillar A $\beta$  may activate surrounding astrocytes and microglia to produce substances that lead to neuritic structural changes in AD.<sup>43</sup> A combination of cellular and molecular mechanisms could be involved in generating the various dendritic abnormalities we observed here. Because the amyloid burden could be extremely high in certain susceptible brain regions, synaptic pathology associated with amyloid deposition could lead to a large-scale and permanent disruption in neuronal circuitry. It is therefore important in the future to develop treatment strategies to prevent and/or alleviate synaptic pathology associated with amyloid deposition.

#### ACKNOWLEDGMENTS

This work was supported by the NIH grants to WBG.

#### REFERENCES

1. ALZHEIMER, A. 1907. Über eine eigenartige Erkyankung der Hirnrinde. *Algermeine Z Psychiatrie* 146–148.
2. TERRY, R.D. & R. KATZMAN. 1983. Senile dementia of the Alzheimer type. *Ann. Neurol.* **14**: 497–506.
3. TERRY, R.D. 1997. The pathology of Alzheimer's disease: numbers count. *Ann. Neurol.* **41**: 7.
4. YANKNER, B.A. 1996. Mechanisms of neuronal degeneration in Alzheimer's disease. *Neuron* **16**: 921–932.

5. LAFERLA, F.M. & S. ODDO. 2005. Alzheimer's disease: abeta, tau and synaptic dysfunction. *Trends Mol. Med.* **11**: 170–176.
6. ARMSTRONG, R.A. 2006. Plaques and tangles and the pathogenesis of Alzheimer's disease. *Folia Neuropathol.* **44**: 1–11.
7. MOTT, R.T. & C.M. HULETTE. 2005. Neuropathology of Alzheimer's disease. *Neuroimag. Clin. N. Am.* **15**: 755–765, ix.
8. BOURAS, C. *et al.* 1994. Regional distribution of neurofibrillary tangles and senile plaques in the cerebral cortex of elderly patients: a quantitative evaluation of a one-year autopsy population from a geriatric hospital. *Cereb. Cortex.* **4**: 138–150.
9. LEWIS, D.A. *et al.* 1987. Laminar and regional distributions of neurofibrillary tangles and neuritic plaques in Alzheimer's disease: a quantitative study of visual and auditory cortices. *J. Neurosci.* **7**: 1799–1808.
10. WEGIEL, J. *et al.* 2001. Shift from fibrillar to nonfibrillar Abeta deposits in the neocortex of subjects with Alzheimer disease. *J. Alzheimer's Dis.* **3**: 49–57.
11. MASLIAH, E., A. MILLER & R.D. TERRY. 1993. The synaptic organization of the neocortex in Alzheimer's disease. *Med. Hypotheses* **41**: 334–40.
12. SCHEFF, S.W. & D.A. PRICE. 1993. Synapse loss in the temporal lobe in Alzheimer's disease. *Ann. Neurol.* **33**: 190–199.
13. GOMEZ-ISLA, T. *et al.* 1997. Neuronal loss correlates with but exceeds neurofibrillary tangles in Alzheimer's disease. *Ann. Neurol.* **41**: 17–24.
14. TERRY, R.D. *et al.* 1991. Physical basis of cognitive alterations in Alzheimer's disease: synapse loss is the major correlate of cognitive impairment. *Ann. Neurol.* **30**: 572–580.
15. MASLIAH, E. *et al.* 1993. Quantitative synaptic alterations in the human neocortex during normal aging. *Neurology* **43**: 192–197.
16. TERRY, R.D. 2000. Cell death or synaptic loss in Alzheimer disease. *J. Neuropathol. Exp. Neurol.* **59**: 1118–1119.
17. SELKOE, D.J. 2002. Alzheimer's disease is a synaptic failure. *Science* **298**: 789–791.
18. KAMENETZ, F. *et al.* 2003. APP processing and synaptic function. *Neuron.* **37**: 925–937.
19. WALSH, D.M. *et al.* 2002. Naturally secreted oligomers of amyloid beta protein potently inhibit hippocampal long-term potentiation *in vivo*. *Nature* **416**: 535–539.
20. D'AMORE, J.D. *et al.* 2003. *In vivo* multiphoton imaging of a transgenic mouse model of Alzheimer disease reveals marked thioflavine-S-associated alterations in neurite trajectories. *J. Neuropathol. Exp. Neurol.* **62**: 137–145.
21. MUCKE, L. *et al.* 2000. High-level neuronal expression of abeta 1-42 in wild-type human amyloid protein precursor transgenic mice: synaptotoxicity without plaque formation. *J. Neurosci.* **20**: 4050–4058.
22. LINDNER, M.D. *et al.* 2006. Soluble Abeta and cognitive function in aged F-344 rats and Tg2576 mice. *Behav. Brain Res.* **173**: 62–75.
23. DODART, J.C., C. MATHIS & A. UNGERER. 2000. The beta-amyloid precursor protein and its derivatives: from biology to learning and memory processes. *Rev. Neurosci.* **11**: 75–93.
24. KOISTINAHO, M. *et al.* 2001. Specific spatial learning deficits become severe with age in beta-amyloid precursor protein transgenic mice that harbor diffuse beta-amyloid deposits but do not form plaques. *Proc. Natl. Acad. Sci. USA.* **98**: 14675–14680.

25. SHEMER, I. *et al.* 2006. Non-fibrillar beta-amyloid abates spike-timing-dependent synaptic potentiation at excitatory synapses in layer 2/3 of the neocortex by targeting postsynaptic AMPA receptors. *Eur. J. Neurosci.* **23**: 2035–2047.
26. KURT, M.A. *et al.* 2001. Neurodegenerative changes associated with beta-amyloid deposition in the brains of mice carrying mutant amyloid precursor protein and mutant presenilin-1 transgenes. *Exp. Neurol.* **171**: 59–71.
27. MASLIAH, E. *et al.* 1996. Comparison of neurodegenerative pathology in transgenic mice overexpressing V717F beta-amyloid precursor protein and Alzheimer's disease. *J. Neurosci.* **16**: 5795–5811.
28. SCHEIBEL, A.B. & U. TOMIYASU. 1978. Dendritic sprouting in Alzheimer's presenile dementia. *Exp. Neurol.* **60**: 1–8.
29. PROBST, A. *et al.* 1983. Neuritic plaques in senile dementia of Alzheimer type: a Golgi analysis in the hippocampal region. *Brain Res.* **268**: 249–254.
30. MASLIAH, E. *et al.* 1991. Patterns of aberrant sprouting in Alzheimer's disease. *Neuron* **6**: 729–739.
31. PHINNEY, A.L. *et al.* 1999. Cerebral amyloid induces aberrant axonal sprouting and ectopic terminal formation in amyloid precursor protein transgenic mice. *J. Neurosci.* **19**: 8552–8559.
32. KNOWLES, R.B. *et al.* 1999. Plaque-induced neurite abnormalities: implications for disruption of neural networks in Alzheimer's disease. *Proc. Natl. Acad. Sci. USA.* **96**: 5274–5279.
33. LE, R. *et al.* 2001. Plaque-induced abnormalities in neurite geometry in transgenic models of Alzheimer disease: implications for neural system disruption. *J. Neuropathol. Exp. Neurol.* **60**: 753–758.
34. BACSKAI, B.J. *et al.* 2003. Four-dimensional multiphoton imaging of brain entry, amyloid binding, and clearance of an amyloid-beta ligand in transgenic mice. *Proc. Natl. Acad. Sci. USA.* **100**: 12462–12467.
35. TSAI, J. *et al.* 2004. Fibrillar amyloid deposition leads to local synaptic abnormalities and breakage of neuronal branches. *Nat. Neurosci.* **7**: 1181–1183.
36. DUFF, K. *et al.* 1996. Increased amyloid-beta<sub>42</sub>(43) in brains of mice expressing mutant presenilin 1. *Nature* **383**: 710–713.
37. HSIAO, K. *et al.* 1996. Correlative memory deficits, Aβ<sub>42</sub> elevation, and amyloid plaques in transgenic mice. *Science* **274**: 99–102.
38. HOLCOMB, L. *et al.* 1998. Accelerated Alzheimer-type phenotype in transgenic mice carrying both mutant amyloid precursor protein and presenilin 1 transgenes. *Nat. Med.* **4**: 97–100.
39. GAN, W.B. *et al.* 2000. Multicolor “DiOlistic” labeling of the nervous system using lipophilic dye combinations. *Neuron* **27**: 219–225.
40. GRUTZENDLER, J., J. TSAI & W.B. GAN. 2003. Rapid labeling of neuronal populations by ballistic delivery of fluorescent dyes. *Methods* **30**: 79–85.
41. SPIRES, T.L. *et al.* 2005. Dendritic spine abnormalities in amyloid precursor protein transgenic mice demonstrated by gene transfer and intravital multiphoton microscopy. *J. Neurosci.* **25**: 7278–7287.
42. BRENDZA, R.P. *et al.* 2003. PDAPP; YFP double transgenic mice: a tool to study amyloid-beta associated changes in axonal, dendritic, and synaptic structures. *J. Comp. Neurol.* **456**: 375–383.
43. EIKELEBOOM, P. *et al.* 2002. Neuroinflammation in Alzheimer's disease and prion disease. *Glia* **40**: 232–239.